# Design and Control of a DC Grid for Railway Stations

Sabah Benamane Siad, Gilney Damm, Lilia Galai Dol, Alexandre de Bernardinis

# Design and Control of a DC Grid for Railway Stations

Sabah SIAD IBISC Laboratory - Paris-Saclay University , France
sabah.siad-benamane@ibisc.univ-evry.fr
Gilney DAMM IBISC Laboratory - Paris-Saclay University , France gilney.damm@ibisc.fr
Lilia GALAI DOL, Efficacity, France, l.galai-dol@efficacity.com
Alexandre DE BERNARDINIS, SATIE TEMA / IFSTTAR, Efficacity, France, alexandre.de-bernardinis@ifsttar.fr;

## Abstract

With growing concerns about environmental issues like climate change, energy efficiency has become crucial. In this framework, the regeneration of the braking energy of trains into electricity is a promising source to highly increase energy efficiency.
The focus of this paper is to Design and Control a Direct Current (DC) Grid integrated in urban railway station, the solution consists in recovering and storing trains braking energy into a hybrid storage system and reusing it for non-railway applications such as loads in a train station and electric vehicles and their recharging plants.
To attain this goal, the main points are power management and voltage control for the DC MicroGrid, and improving the dynamic performance of the system. These are obtained by controlling the energy storage system.

## 1. Introduction

The consumption of energy is increasing constantly in the word. In the meantime, limited availability of conventional sources has encouraged a better use of available energy and to develop alternatives for generating power.
Among others, the Braking Energy Recovery System (BERS) power is an important energy efficiency issue. During the last decade, considerable progress has been made of electric traction due to evolving of Power electronics. These innovations have made it possible a large range of regeneration of the train braking energy, and offer a very attractive way to reduce the energy consumption of urban railway stations.However, the electricity production from these sources is strongly variable with very high transients (see [1] to [4]).
This energy is naturally available when the train uses electric brakes to slow down its engines, instead of using mechanical brakes. It is then necessary to design a hybrid Storage system to limit power losses and store the excess of braking energy. Nevertheless, this system must take into account several operating constraints (see [2] and [5]). The stored energy can be used to supply the railway station load for many hours.
The energy coming from urban trains is available in a DC grid, the storage system being also DC; it is then natural to develop a control strategy in a DC node (see [2], [6] and [7]).
The model of each component of the DC MicroGrid has to be developed. In this paper, we propose through a power electronics study to analyse the dynamic behaviour of the system and to simulate the electric power flow and to optimize the storage device size, lifetime and control algorithm (see [3] and [8]).
This paper is organized as follows.
Section II describes Braking Energy Recovery System Configuration. Section III deals with modelling of the source and associated power electronics. Section IV concerns the Energy storage system (lithium ion and Supercapacitor) where all aspects related to modelling, control and integration are addressed
Section V presents the power plant in the DC grid Section VI provides simulation results about the system. In section VII conclusions are provided.

## 2. BERS Configuration

The braking energy recovery system consists of a DC/DC converter which is connected in parallel to an existing substation, with an Energy Storage System (ESS) which permits to store the energy.
As said before, since all elements are in DC, we have chosen to build a DC grid. As shown in Fig1, the proposed system consists of train residual

braking energy as source, energy storage elements such as super-capacitors and batteries, DC loads and grid-tied converter. The train residual braking energy converter is a 1 MW buck converter Energy storage elements play an important role for the entire power management of the DC micro-grid. They ensure a secured grid network, provide high quality power and maintain common DC grid voltage constant [5].

Bidirectional converters are used to charge or discharge the energy storage elements, while an inverter is used to feed railway station ([14] [20]).

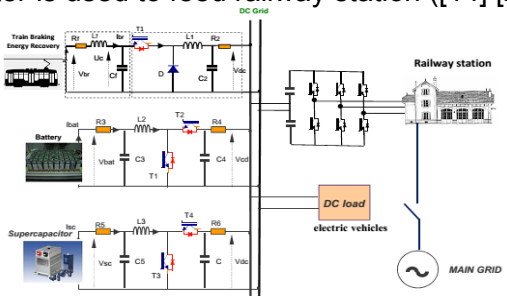


Fig. 1. System Configuration

For modeling the converters' switches it will be included small resistances ($Ro_1$, $Ro_2$, $Ro_3$ $Ro_4$, $Ro_5$ and $Ro_6$,) when they are driving, so the conduction losses are taken into account.

# 3. BERS Modeling

## 3.1. Braking Energy Recovery as sources

The considered railway system works in 750 V to recover energy by regenerative braking [1]. We in tegrate a LC filter due to very fluctuating current as shown below.

## 3.2. DC/DC buck Converter

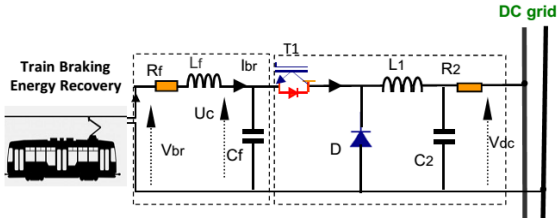


Fig. 2. DC/DC Buck Converter Circuit

The DC/DC converter topology used is the buck (Fig. 2) the analytical method to model such converter is a state-variable-averaging method ([19], [21]), that can be expressed as:

$$\begin{cases} \dot{x} = Ax + Bu = [A_1 \cdot u_1 + A_2 \cdot (1-u_1)]x + [B_1 \cdot u_1 + B_2 \cdot (1-u_1)]u \\ y = Cx = [C_1 \cdot u_1 + C_2 \cdot (1-u_1)]x \end{cases} \quad (1)$$

Where x denotes the system states that have been averaged over one switching cycle. y is the output vector, u is control vector, A the state matrix, B the input matrix and C the output matrix.

Thus, we have: in the interval [0, $u_1T$], that T1 is closed and in the interval [$u_1T$, T], T1 is open .

$$A = \begin{bmatrix} 0 & 0 & -\frac{1}{C_f} & -\frac{u_1}{C_f} \\ 0 & -\frac{1}{R_2 C_2} & 0 & \frac{1}{L_1} \\ -\frac{1}{L_f} & 0 & \frac{R_f}{L_f} & 0 \\ \frac{1}{L_1} & -\frac{1}{L_1} & 0 & \frac{-u_1 R_{01} - (1-u_1) R_{02}}{L_1} \end{bmatrix} \quad B = \begin{bmatrix} 0 & 0 \\ 0 & \frac{1}{R_2 \cdot C_2} \\ \frac{1}{L_f} & 0 \\ 0 & 0 \end{bmatrix}$$

$$C = [0 \quad 0 \quad 0 \quad 1] \quad (2)$$

The following equations can be obtained

$$\begin{cases} \frac{dU_C}{dt} = -\frac{1}{C_f} i_{Lf} - \frac{u_1}{C_f} i_{L1} \quad \ldots\ldots 1 \\ \frac{dV_{C2}}{dt} = -\frac{1}{R_2 C_2} V_{C2} + \frac{1}{L_1} i_{L1} + \frac{1}{R_2 C_2} V_{dc} \quad \ldots\ldots 2 \\ \frac{di_{Lf}}{dt} = -\frac{R_f}{L_f} i_{Lf} - \frac{1}{L_f} U_C + \frac{1}{L_f} V_{br} \quad \ldots\ldots 3 \\ \frac{di_{L1}}{dt} = \frac{1}{L_1} U_C - \frac{1}{L_1} V_{C2} + \frac{-u_1 R_{01} - (1-u_1) R_{02}}{L_1} i_{L1} \quad \ldots\ldots 4 \end{cases} \quad (3)$$

## 3.3. Control law

The braking of the train increases the energy, therefore an overvoltage in the catenary. The control strategy is to reduce this voltage to the nominal voltage of the grid (750V) by recovering this energy through the converter. Here the control target is to control voltage at $V_{br}$, it means to control $U_c$ value ([24], [28]).

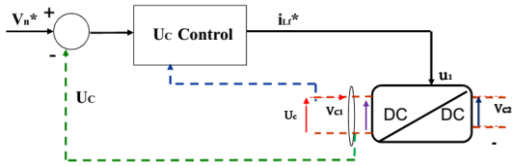


Figure: 3 DC/DC Buck

The reference value for Uc is the nominal voltage Vn*; used in the first equation. In order to assign Vn* reference value to Uc, an iLf* reference value for iLf is designed by backstepping technique. Consider the system (3) and the desired equilibrium points $U_C^*$ , $V_{C2}^*$ , $i_{Lf}^*$. and $i_{L1}^*$ (4)

Where $V_n^*$ is given and $i_{Lf}^*$ is a function of $V_n^*$.

The $V_{C2}$ and $i_{L1}$ variables will be the zero dynamic, which will be chosen to converge to a desired set.

Then taking the current $i_{L1}$ and (ideally) the DC grid voltage value:

$$i_{Lf}^* = -K_1 C_f \left(U_C - V_n^*\right) - \overline{K_1} C_f \alpha_1 + \frac{u_1}{C_f} i_{L1} \quad (5)$$

In order to assign $V_{C1}^*$ reference value to $V_n^*$ the

reference $i_{Lf}^{*}$ value for is $i_{Lf}$ selected as in equation 5 where $\alpha_1$ is governed by equation

$$\dot{\alpha}_1 = K_1^{\alpha}\left(U_C - V_n^{*}\right) \quad (6)$$

Consequently, the first equation of (3) becomes

$$\dot{U}_C = -K_1\left(U_C - V_n^{*}\right) - K_1^{\alpha}\left(U_C - V_n^{*}\right) \quad (7)$$

According to the output choice

$$y_1 = U_C \quad (8)$$

Let the $u_1$ control input be

$$u_1 = \frac{1}{K_3 i_{L1}}\left[\left(K_3 - \frac{R_f}{L_f}\right)i_{Lf} + K_1 K_3 C_f\left(U_C - V_n^{*}\right) - \frac{1}{L_f}\left(U_C - V_{br}\right) + \overline{K_1} K_3 C_f \alpha_1 + K_3 \alpha_3\right] \quad (9)$$

Then the system asymptotically converges to the equilibrium points (4). The controlled equilibrium is then locally asymptotically stable, with the following condition to be respected:

$$K_3 i_{L1} \neq 0 \quad (10)$$

We operate in Continuous conduction mode, and then we may select the value for inductor $L_1$ for which the inductor current is greater than zero at all times and under all allowed operating conditions of the converter. Then, the condition (10) is satisfied.

The Lyapunov function is taken for the two selected states

$$V_{1,3} = \frac{1}{2}\left(U_C - V_n^{*}\right)^2 + \frac{\overline{K_1}}{2K_1^{\alpha}}\alpha_1^2 + \frac{1}{2}\left(i_{Lf} - i_{Lf}^{*}\right)^2 + \frac{\overline{K_3}}{2K_3^{\alpha}}\alpha_3^2 \quad (11)$$

where $\alpha_3$ is governed by equation

$$\dot{\alpha}_3 = K_3^{\alpha}\left(i_{Lf} - i_{Lf}^{*}\right) \quad (12)$$

and its derivative is calculated in order to develop a proper controller:

$$\dot{V}_{1,3} = -K_1\left(U_C - V_n^{*}\right)^2 - K_3\left(i_{Lf} - i_{Lf}^{*}\right)^2 \quad (13)$$

The Lyapunov derivative is semidefinite negative, but using Barbalat's lemma we can state that the system is asymptotically stable.

Let us now move the focus to the zero dynamics. Taking

$$\dot{y}_1 = U_c \equiv V_n^{*} \quad (14)$$

Consequently

$$i_{Lf} \equiv i_{Lf}^{*} = \frac{V_{br} - V_n^{*}}{R_f} \quad (15)$$

We can rewrite the zero dynamics equations as

$$\dot{i}_{L1} = \left[\frac{R_{02}}{L_1} + \frac{\left(R_{02} - R_{01}\right)u_1}{L_1}\right]i_{L1} + \frac{1}{L_1}\left(U_C - V_{C2}\right) \quad (16)$$

$$\dot{V}_{C2} = -\frac{1}{R_2 C_2}V_{C2} + -\frac{1}{L_1}i_{L1} + \frac{1}{R_2 C_2}V_{dc} \quad (17)$$

The equations 16 and 17 are a linear stable first order system, which means that according to it the equilibrium point will be given by $i_{Lf}$ and $V_{DC}$ values, and then the system is always stable.

# 4. Energy Storage System modeling

The hybrid storage system adopts the advantage of both technologies, high power density from the supercapacitor and high energy density from the battery.

The proposed Hybrid storage consists of Lithium-ion battery and a supercapacitor ([12], [13]. [15]).

## 4.1 Battery modeling

### 4.1.1 Simulink model

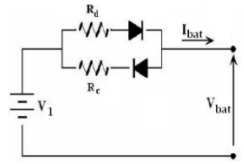


Figure 4 Resistive Thevenin battery model scheme

The model chosen for a Lithium ion Battery is based on the resistive Thevenin model. It holds on the estimation of the battery state-of-charge.

The battery is considered as a voltage generator ([9], [10], [11]).

### 4.1.2 Bidirectional Boost Converter.

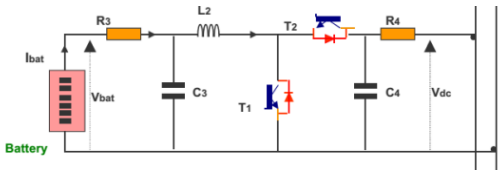


Figure 5 DC/DC BOOST Converter Circuit

We have two structures for the above converter. In the first one, the current branch receives energy in a positive voltage ([19], [21]).

In the second structure, branch current supplies power in a positive voltage. The reversal of power transfer is obtained by changing the direction of the current. Similarly to section 2, the following equations can be obtained. In the first interval [0, $u_2$T], T1 closes and T2 opens. In the interval [$u_2$T, T], T1 opens and T2 closes. Where u2 denotes the duty ratio of the switches.

Noteworthy that in these driving modes, if $0<u_2<0.5$ the power goes from the low side to the high side, and if $0.5 <d<1$ the power goes the other way. We select three state variables, the voltages on the capacitors $C_3$ and $C_4$ and the current in the inductance $L_2$.

$$\begin{cases} \dfrac{dV_{C3}}{dt} = -\dfrac{1}{R_3C_3}V_{C3} - \dfrac{1}{C_3}i_{L2} + \dfrac{1}{R_3C_3}V_{BAT} \text{.....1} \\ \dfrac{dV_{C4}}{dt} = -\dfrac{1}{R_4C_4}V_{C4} + \dfrac{1-u_2}{C_4}i_{L2} + \dfrac{1}{R_4C_4}V_{dc} \text{.....2} \\ \dfrac{di_{L2}}{dt} = \dfrac{1}{L_2}V_{C3} - \dfrac{1}{L_2}V_{C4} + \dfrac{-u_2R_{03} - (1-u_2)R_{04}}{L_2}i_{L2} \text{.....3} \end{cases} \quad (18)$$

**4.1.3**

## Control law

Now we have to set the regulation loops correctly. There are two steps of regulation that have to be set over our system; each of them is having its own specificity ([27], [28]).

The first is to respond to the need of a power transfer from the network to the storage system and vice-versa. The second is to set keep currents or voltages in chosen boundaries so as not to stress or destroy electric components.

Battery current and voltage regulation consists in a cascade control: there will be an inner current loop and an outer voltage loop.

First, we consider the inner current loop designed to control the converter that directly stabilizes the network (see [15]). Then, we have to consider the control of the DC-DC interface. The current Idc in the DC grid is directly linked to the current from the storage systems Ist (see equation 36), and this current has to be supplied or absorbed at the same time and with the same amplitude as IL2 through the control of the converter switches. This is why the Ist reference of storage current is defined by the amount of power the operator wants to transfer to or from the battery given by Ibat_ref (how to compute Pbat_ref is shown in section 5).

This procedure is used when the state of the charge (SOC) is between 40% and 80%.

In the second step, the control objective is to keep the battery from being overcharged or undercharged, either of which significantly reduces the battery's life. Typically, a deep-cycle battery should not be discharged past 30% or charged past 100%, and then the current will be used for controlling the desired capacitor voltage $V_{C3}^*$ .

In our study, the system is sized such that the battery and supercapacitor stay in 40%<SOC<80%, so we work in the linear phase of the battery.

Consider the system (18) and the desired equilibrium points $V_{C3}^*$, $V_{C4}^*$ and $I_{L2}^*$ (19)

Where $I_{L2}^*$ is given by the current in the DC grid (see section 5).

According to the output choice $y_2 = I_{L2}$ (20)

From equation of the current (18) let the $u_2$ control input be as in (21**):**

$$u_2 = \frac{1}{V_{C4} + (R_{04} - R_{03})i_{L2}}\left[-V_{C3} + V_{C4} - R_{04}i_{L2} + L_2K_6(i_{L2} - i_{L2}^*) + L_2\overline{K_6}\alpha_6\right] \quad (21)$$

the following condition needs to be respected:

$$V_{C4} + (R_{04} - R_{03})i_{L2} \neq 0 \quad (22)$$

where $i_{L2}^*$ be the desired value for the inductance c urrent, and $\alpha_4$ is governed by equation:

$$\dot{\alpha}_6 = K_6^{\alpha}(i_{L2} - i_{L2}^*) \quad (23)$$

The closed loop dynamics will then be

$$\dot{i}_{L2} = -K_6(i_{L2} - i_{L2}^*) - \overline{K}_6\alpha_6 \quad (24)$$

The Lyapunov function (25) is used to analyze the behavior for the two selected states

$$V_{4,6} = \frac{1}{2}(V_{C3} - V_{C3}^*)^2 + \frac{1}{2}(i_{L2} - i_{L2}^*)^2 + \frac{\overline{K_6}}{2K_6^{\alpha}}\alpha_6^2 \quad (25)$$

$V_{C3}^*$ being the value for the capacitor voltage.

$$V_{C3}^* = V_{bat} - R_2i_{L2}^* \quad (26)$$

Its derivative is calculated as:

$$\dot{V}_{4.6} = -K_4(V_{C3} - V_{C3}^*)^2 - K_6(i_{L2} - i_{L2}^*)^2 \leq 0 \quad (27)$$

The Lyapunov derivative is semidefinite negative, but utilizing Barbalat's lemma we can state that the system is asymptotically stable.

Analyzing it when $i_{L2}^*$ equilibrium point is reached:

$$\frac{dV_{C4}}{dt} = \frac{1}{R_4C_4}(V_{DC} - V_{C4}) + \frac{1}{C_4}\left[\frac{V_{C3} - R_{03}i_{L2}^*}{V_{C4} + (R_{04} - R_{03})i_{L2}}\right]i_{L2}^* \quad (28)$$

The analysis is performed using the linearization around the equilibrium points in order to check stability:

$$-\frac{V_{C3}}{R_{03}} << (I_5) << \frac{V_{C3}}{R_{03}} \quad (29)$$

The condition 29 being always satisfied, the system is stable.

A nominal current of the Battery $I_5 = C_5 / 5hours$ denotes the constant current of charge and discharge for five hours

Where the C rate is the capacity of the battery of delivering so much current for so many hours

## 4.2 Supercapacitors

## 4. 2.1 Equivalent model

The following figure represents the equivalent circuit of the three-branch model: [16], [17]. [18].

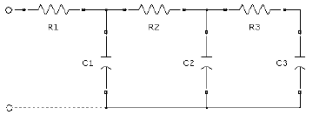


Figure 6: Equivalent circuit of Supercapacitor,

### .4.2.2 Bidirectional Boost Converter.

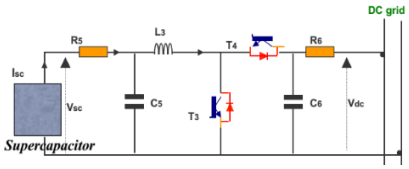


Figure 7: DC/ Bidirectional Converter Circuit

### 4.2.3 .Control law

As in the battery, the current will be used for control the desired capacitor current.

$$\begin{cases} \dfrac{dV_{C5}}{dt} = -\dfrac{1}{R_5 C_5} V_{C5} - \dfrac{1}{C_5} i_{L3} + \dfrac{1}{R_5 C_5} V_{BAT} \text{.....1} \\ \dfrac{dV_{C6}}{dt} = -\dfrac{1}{R_6 C_6} V_{C8} + \dfrac{1-u_n}{C_6} i_{L3} + \dfrac{1}{R_6 C_6} V_{dc} \text{.....2} \\ \dfrac{di_{L3}}{dt} = \dfrac{1}{L_3} V_{C5} - \dfrac{1}{L_3} V_{C6} - \dfrac{-u_3 R_{05} - (1-u_3) R_{06}}{L_3} i_{L3} \text{.....3} \end{cases} \quad (30)$$

Consider the system (30) and the desired equilibrium points Vc5*, Vc6* and IL3* (31)

Where $i_{L3}^{*}$ is given by the current in the DC grid (see section 5). According to the output choice

$$y_2 = i_{L3} \quad (32)$$

From equation of the current (30) Let $u_3$ the control input be

$$u_3 = \frac{1}{V_{C6} + (R_{06} - R_{05}) i_{L3}} \left[ -V_{C5} + V_{C6} - R_{06} i_{L3} + L_2 K_9 \left( i_{L3} - i_3^{*} \right) + L_3 \overline{K}_9 \alpha_9 \right] \quad (33)$$

The stability analysis is same as in the battery.

## 5. Analysis of the Proposed DC MicroGrid

### 5.1 Power Flow

The power flow in the MicroGrid is shown in Fig. 8. It is the sum of the output power of the train residual braking energy, the consumption and the storage. It is defined as follow (see [10] and [20]).

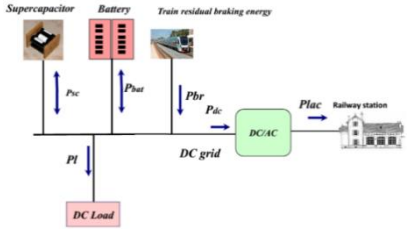


Fig 8: Power Flow of DC MicroGrid

$$P_{DC} = P_{br} - P_{load} - |P_{ST}| \quad (34)$$

$$P_{ST} = P_{bat} + P_{sc} \quad (35)$$

$P_{br}$: Braking power, $P_{ST}$: Storage system power, $P_{bat}$ Battery power, Supercapacitor power, $P_l$: Load power and $P_{DC}$: DC MicroGrid power.

### 5.2 Power Control of an Energy Storage

The train residual braking energy is strongly time-varying with several high peaks, and needs to be dealt with properly to ensure that electrical devices connected to the grid do not receive too few or too much power. The DC grid is connected to the AC grid ([22]).

The residual braking energy serves in priority to supply the train station through the inverter. The energy storage elements can switch between charge and discharge mode in order to maintain the DC grid power balance.

Supercapacitor undertakes the sudden peak of power while the battery undertakes the demands of large amounts of power for long time periods. In this work strong currents are minimized in the battery aiming at maximizing its lifetime.

In previous sections we set a control law for charging and discharging the battery and supercapacitor, in this section we define the references for these controllers.

We proceeded as follow: according to a varying load demand, the energy storage element realizes a power balance. From equation (35):

$$|P_{load} - P_{br}| = |P_{ST}| = P_{DC\_ref} \quad (36)$$

$$\frac{dV_{dc}}{dt} = \frac{1}{C_{dc}} \left[ \frac{1}{R_2} (V_{C2} - V_{dc}) + \frac{1}{R_4} (V_{C4} - V_{dc}) + \frac{1}{R_6} (V_{C6} - V_{dc}) - i_{load} \right] = \frac{P_{DC\_ref}(t)}{C_{DC} V_{DC}} \quad (37)$$

Based on the physical characteristics of the storage components, and in particular on the current limitations from the battery, we propose to decompose the power reference in two components, a fast and a fundamental (slow).

The fundamental component will be the reference power for the battery, while the fast fluctuating component will be the reference power for the supercapacitor ([23] an [25]).

The two components must be chosen such to keep sufficient time-scale separation between the power and the voltage control objectives, and to assure that the battery does not need to react faster than its specifications. In this way, the lifespan of the battery is seriously augmented ([27]).

A low-pass filter (LPF) with a cutoff frequency ($f_c$) of 3 Hz is used to decompose the power reference, in other words the LPF provides for the battery

current control loop a ripple-free (slow) reference signal ($I_{bat\_ref}$) and for the supercapacitor current control loop a rippled (fast) reference signal ($I_{sc\_ref}$)

$$P_{DCref}(t) = P_{\_long} + P_{\_fast} \quad (38)$$

$I_{bat\_ref} = \frac{P_{\_long}}{V_{dcnom}}$ acts to maintain the balance of power

$I_{sc\_ref} = \frac{P_{\_fast}}{V_{dcnom}}$ acts to dampen oscillations

# 6. Simulation result

In this section, some simulations are conducted:

Table 1 Parameters for battery

| Parameters | Values |
|---|---|
| V_cell | 3.2 V |
| Nominal power | 1 MW |
| Duration of power compensation | 5h |
| C_10 | 15000A |
| I_10 | 1500A |
| LAB Electrochemical process efficiency | K = 0.75 |
| LAB self-discharge rate | D = 1e-5 |
| Step_sec | 3600 |
| Nb_serie/ Nb parallel | 100/1 |

Table 2 Parameters for Supercapcitor

| | | | |
|---|---|---|---|
| *R1* | *0.3 * ESR* | *C1* | *0.4 * C* |
| *R2* | *0.2 * ESR* | *C2* | *0.414 * C* |
| *R3* | *0.5 * ESR* | *C3* | *0.16 * C* |
| Voltage across the SC | | 1000 V to 2000 V | |
| Discharge Ratio Desired/Limit | | d=50% | |
| Required Demanded Power | | 1 MW to over 2MW | |
| P_required | | 1MW | |
| Capacitance | | 2600F | |
| Stable Operating Voltage | | 2.70V | |
| ESR | | 0.35mΩ | |
| Time Constant | | 0.9 | |
| Thermal Operating Conditions | | 40°c to +70°c | |
| Lifetime expected to exceed | | 500,000 operating cycles 10 year expected life | |

Table 3 simulation parameters

| | | | | | |
|---|---|---|---|---|---|
| $R_{o1} = R_{o2}$ | 0.001Ω | $R_{o1} = R_{o2}$ | 0.001Ω | $R_{o1} = R_{o2}$ | 0.001Ω |
| $R_1$ | 0.25Ω | $R_3$ | 0.1Ω | $R_5$ | 0.1Ω |
| $R_2$ | 0.001Ω | $R_4$ | 0.001Ω | $R_6$ | 0.001Ω |
| $C_1$ | 0.15 F | $C_3$ | 0.1 F | $C_5$ | 0.2 F |
| $C_2$ | 0.02 F | $C_4$ | 0.02 F | $C_6$ | 0.02 F |
| $L_1$ | 0.05 H | L2 | 0.0033 H | $L_3$ | 0.0033 H |
| Pn | 1MW | Pn | 1MW | Pn | 1MW |

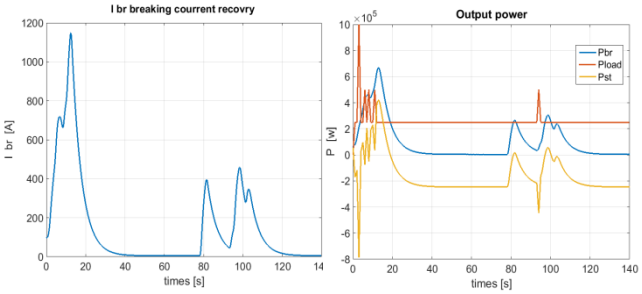


Fig 9: - Train residual braking current and power

In Fig. 9 one can see the strong power (right) and respective current (left) from the braking. This power shape is instantaneously absorbed by the supercapacitor (Psc), such that the battery can stay rather unchanged during the whole time. As a consequence its lifespan is significantly increased. The battery can then provide most of the energy demanded by the load, allowing long term planning, and the use of weather forecast and load predictions in the higher level algorithms

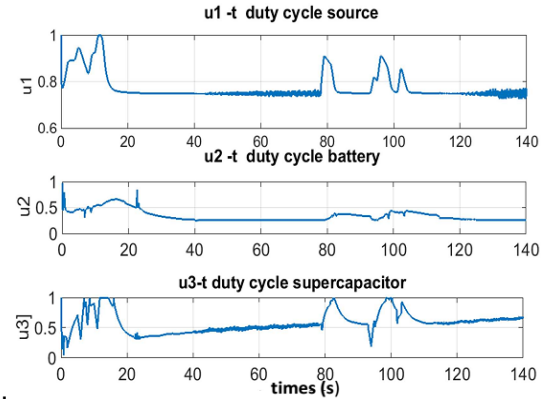


Figure10 control inputs $u_1$,$u_2$ and $u_3$

The control inputs are smooth except in the case of fast power variations of different elements of the DC MicroGrid

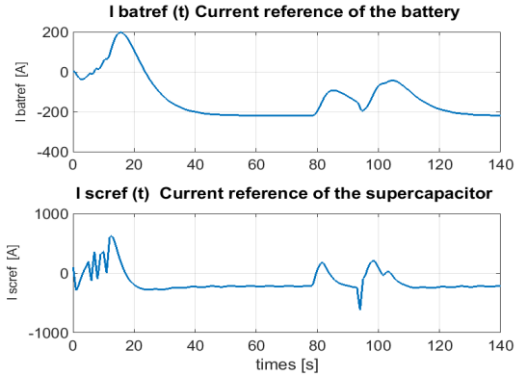


Figure 11 Reference current components

In Fig. 11 can see the variations of the two components of the power reference provided by storage, the slow reference and the fast reference.

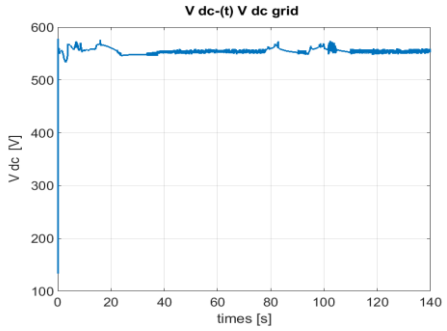


Figure 12 DC MicroGrid voltage

We can see in Figure 12 that the controller always keeps $V_{dc}$ close to its nominal value. The control strategy is then shown to successfully operate in a wide range of situations

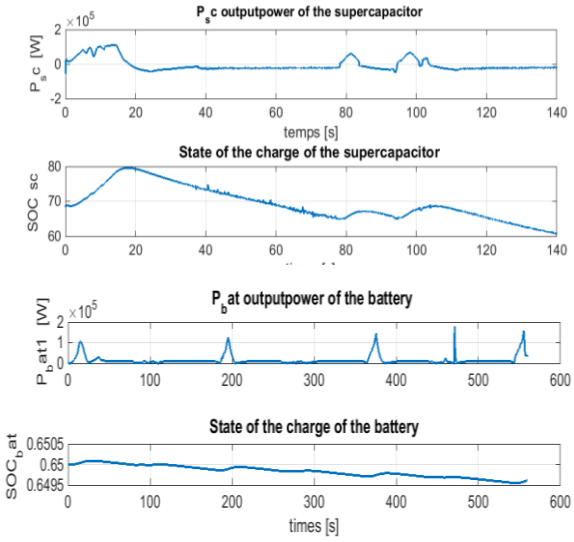


Figure 13 Output power and state of the charge of the battery and supercapacitor

Figure 13 illustrate Output power and the state (SOC) of the charge for the battery and supercapacitor, we can see the supercapacitor charge and discharge very fast to meet a peak power demand and battery discharge slowly to secure power plant and to maintain voltage in dc grid

## 6. Conclusion

The need to improve energy efficiency has led to developing braking energy recovery from trains. To attain this goal it was designed a flexible integration strategy of such sources to the network based on “Plug and play systems” philosophy, using a hybrid storage system composed of a battery and a supercapacitor connected to a DC grid.

In, this paper each converter in this system is modeled in order to study the dynamic behavior of the overall system. The power management strategy and the nonlinear control are developed in for the DC distribution system recovering the DC train braking energy.

The regulated sources (storage) are used to keep the DC voltage and guarantee the balance between generation and energy consumption; this is obtained by an algorithm applied in these storage elements that tracks the DC voltage, and injects electric power into the DC network.

This paper is based on realistic characteristics of the grid’s element, and was focused on proposing easily implementable control algorithms.

Simulation results illustrate our claims, and the good behavior of each element and the overall interconnected system. In this paper, we chose to work in the linear part of the battery and the supercapacitance, which allowed us to regulate the voltage of $V_{dc}$ without stressing these elements. This approach offers advantages for the network and the storage.

In future works, we will take into account the nonlinear part of the battery and supercapacitor, and regulate $V_{dc}$ by the inverter; afterwards we will compare the two methods. Real size experiments are under construction.

## References

[1] L. Galai Dol, A. De Bernardinis “AC or DC grid for urban railway station?” PCIM Europe 2016,

[2] Heng Li, Jun Peng, Weirong Liu and Zhiwu Huang” Stationary Charging Station Design for Sustainable Urban Rail Systems: A Case Study at Zhuzhou Electric Locomotive Co., China” Sustainability 2015,

[3] T. Ahmed, A. Mohamed Ahmed, A. Mohamed Osama, “DC microgrids and distribution systems: An overview” Electric Power System Research, Elsevier, 2015.

[4] L. Abrahamsson, T. Kjellqvist, S.Ostlund “HVDC Feeder Solution for Electric Railways”

[5] Sarah Nasr, Marc Petit, Marius Iordache, Olivier Langlois “Stability of DC micro-grid for urban railway systems “International Journal of Smart Grid and Clean Energy

[6] E. Jimenez, M. J. Carrizosa, A. Benchaib, G. Damm, and F. LamnabhiLagarrigue, “A new generalized power flow method for multi connected DC grids,” International Journal of Electrical Power and Energy Systems, vol. 74, pp. 329 – 337, 2016

[7] M. Jiménez Carrizosa, F. Dorado Navas, G. Damm , A. Benchaib and F. Lamnabhi-Lagarrigue,

Optimal power flow in multi-terminal HVDC grids with offshore wind farms and storage devices, International Journal of Electrical Power and Energy Systems, Fév. 2015

[8] Fernando A Inthamoussou, Student Member, IEEE, Jordi Pegueroles-Queralt, and Fernando D. Bianchi." Control of a Supercapacitor Energy Storage System for Microgrid Applications" IEEE TRANSACTIONS ON ENERGY CONVERSION, VOL. 28, NO. 3, SEPTEMBER 2013

[9] GERGAUD.O,ROBIN.G, MULTON.B, BEN AHMED.H, SATIE "Energy modeling of a lead-acid battery within hybrid wind/photovoltaic systems", - Brittany Branch, ENS de Cachan - Ker Lann Campus, 2003

[10] Barton, J., Infield, D., "Energy storage and its use with intermittent renewable energy" IEEE Transactions on Energy Conversion, v 19, n 2, p 441-448, June 2004.

[11] Bhatia, R.S., Singh, B., Jain, D.K., Jain, S.P., (2008)"Battery energy storage system based power conditioner for improved performance of hybrid power generation"2008 Joint International Conference on Power System Technology POWERCON and IEEE Power India Conference, POWERCON 2008

[12] Roberts, Bradford P.(2001) "Energy storage applications for large scale power protection systems" Proceedings of the IEEE Power Engineering Society Transmission and Distribution Conference, v 2, p 1157-1160, 2001

[13] Krajacic, G., Duic, N., Vad Mathiesen, B., Da Graça Carvalho, M., (2010)"Smart energy storages for integration of renewable in 100% independent energy systems" Chemical Engineering Transactions, v 21, p 391-396, 2010.

[14] Ji-Heon Lee, Hyun-Jun Kim, Byung-Moon Han, Yu-Seok Jeong, Hyo-Sik Yang and Cha: (2011) "DC Micro-Grid Operational Analysis with a DetailedlSimulation Model for Distributed Generation". Journal of Power Electronics Vol 11, N°3 Mai 2011.

[15] Ongaro.F, Saggini.S, and Mattavelli.P (2012) "Li-Ion Battery-Supercapacitor Hybrid Storage System for a Long Lifetime, Photovoltaic-Based Wireless Sensor Network" IEEE TRANSACTIONS ON POWER ELECTRONICS, VOL. 27, NO. 9, SEPTEMBER 2012

[16] M.E. Glavin, Paul K.W. Chan, S. Armstrong, and W.G Hurley (2008)"A Stand-alone Photovoltaic Supercapacitor Battery Hybrid Energy Storage System" 13th Power Electronics and Motion Control Conference (EPE-PEMC 2008

[17] Miller JM., Nebrigic. D, Everett.M (2006)"Ultra capacitor Distributed Model Equivalent Circuit for Power Electronic Circuit Simulation". Maxwell Technologies Inc. San diego. CA. Ansoft Leading Insights Workshop. July 2006.

[18] Lifshitz.D and Weiss.G, (2015)"Optimal control of a capacitor-type energy storage system," Automatic Control, IEEE Transactions on, vol. 60, pp. 216–220, Jan 2015.

[19] S. Sanders, J. Noworolski, X. Liu, and G. C. Verghese,"Generalized averaging method for power conversion circuits," Power Electronics, IEEE Transactions on, vol. 6, pp. 251–259, Apr 1991.

[20] Iovine.A, Benamane Siad.S, Benchaib.A and Damm.G, (2014) "Management of the Interconnection of Intermittent Photovoltaic Systems through a DC Link and Storage", ERCIM, European Research Consortium for Informatics and Mathematics, number 97. April 2014

[21] Merdassi.A. (2010) « La modélisation Automatique pour l'électronique de puissance » Editions Universitaires Européennes.2010.

[22] Dragicevic.T, Vasquez.J, Guerrero.J, and. Skrlec.D, (2014)"Advanced LVDC Electrical Power Architectures and Microgrids: A step toward a new generation of power distribution networks.," Electrification Magazine,IEEE, vol. 2, pp. 54–65, March 2014.

[23] Guerrero, P. C. Loh, T.-L. Lee, and M. Chandorkar, (2013)"Advanced Control Architectures for Intelligent Microgrids Part II: Power Quality,Energy Storage, and AC/DC Microgrids," Industrial Electronics, IEEE

[24] Generalized power flow method for multi connected Marx.D, Magne. P, Nahid-Mobarakeh. B, Pierfederici. S, and Davat. B,"Large (2012) "Signal Stability Analysis Tools in DC Power Systems With Constant Power Loads and Variable Power Loads"; A Review," PowerElectronics, IEEE Transactions on, vol. 27, pp. 1773–1787, April 2012.

[25] Hamache. D, Fayaz. A, Godoy.E, and Karimi.C , (2014) "Stabilization of a DC electrical network via backstepping approach,"in Industrial Electronics (ISIE), 2014 IEEE 23rd International Symposium on, pp. 242–247, June 2014.

[26] Qobad.S. Tomislav.D, Juan Carlos Vasquez.Q, Josep M.G (2014)." Modeling, Stability AProceedings of the 2014 IEEE International Energy Conference (ENERGYCON)nalysis and Active Stabilization of Multiple DC-Microgrids Clusters"

[27] Chen.Y; Benchaib. A, Damm. G, and F. LamnabhiLagarrigue, (2014) "Control induced explicit time-scale separation to attain DC voltage

[28] A. Iovine, S. B. Siad, G. Damm, E. De Santis, M. D. Di Benedetto, "Nonlinear Control of a DC MicroGrid for the Integration of Photovoltaic Panels", https://arxiv.org/abs/1607.08489, IEEE Transactions on Automation Science and Engineering, to appear, 2017